inter·noise 2023
CHIBA,GREATER TOKYO 20-23 AUGUST

Reduction of Flow-Induced Trailing Edge Noise of Semi-Infinite Flat Plate by Structural Resonance

Irsalan ARIF[1]
Department of Aerospace Engineering, College of Aeronautical Engineering
National University of Sciences and Technology (NUST), Pakistan

Randolph C. K. LEUNG[2]
Department of Mechanical Engineering, The Hong Kong Polytechnic University
Hung Hom, Kowloon, Hong Kong, P. R. China

Muhammad Rehan NASEER[3]
Department of Mechanical Engineering, The Hong Kong Polytechnic University
Hung Hom, Kowloon, Hong Kong, P. R. China

Shuaib SALAMAT[4]
Department of Aerospace Engineering, College of Aeronautical Engineering
National University of Sciences and Technology (NUST), Pakistan

ABSTRACT

A unique method for the reduction in flow-induced trailing edge noise scattering for a semi-infinite thin plate is proposed by utilizing short flexible panels mounted on the surface of the plate. The proposed configuration differs from conventional cantilevered elastic trailing edges due to the limitations of their structural integrity and applicability. The key idea is to design short panels that vibrate in structural resonance under the fluid loading for absorbing the energy from the flow to sustain their vibration. A time-domain direct aeroacoustic simulation coupled with structural dynamics is carried out at a low Reynolds number of 50,000 to explore the aeroacoustic-structural interactions. The effectiveness of noise reduction of the designed configuration is analyzed by comprehensive aeroacoustic analysis where a significant noise reduction is observed for the plate mounted with three flexible panels without any adverse effects on the plate aerodynamics. The structural analysis shows a systematic vibration pattern for all the panels which clearly indicates the presence of complex fluid-structural interaction under resonance conditions. Design strategy of the proposed configuration along with its limitations are also discussed.

1. INTRODUCTION

Trailing edge scattering noise is a significant aerodynamic noise source in practical engineering applications, such as aircraft wings, turbine blades, airframe, and rotors [1–4]. The generation

[1]arsalan_sayani@cae.nust.edu.pk
[2]mmrleung@polyu.edu.hk (Corresponding author)
[3]rehan.naseer@connect.polyu.hk
[4]ssalamat@cae.nust.edu.pk

of trailing edge noise typically involves the interaction between flow turbulence and a geometric discontinuity, leading to unsteady flow that creates surface pressure fluctuations. These fluctuations are scattered and propagated to the far field as trailing edge noise [5].

Due to the importance of this issue, which restricts the operational capabilities of various aerodynamic devices, researchers have proposed and developed different methods to suppress trailing edge noise [6–8]. Bae et al. [9] conducted numerical investigations on a flat plate with an elastic cantilever end at a low Reynolds number (Re) and observed both noise reduction and amplification at the natural frequency of the elastic trailing edge. Nardini et al. [10] also performed a numerical study on a similar configuration with external excitation and observed noise reduction or amplification depending on the relative phase and amplitude of the incident flow field and structural motion. The impact of a cantilevered poroelastic plate on noise scattering has also been extensively studied, demonstrating some noise reduction across a range of frequencies [11]. Recently, Kolb and Schaefer [12] examined the aerodynamic and acoustic effects of fully membrane airfoils/plates. While the existing methods have achieved varying degrees of noise reduction under specific flow conditions, they are limited by certain structural constraints. Specifically, flexible trailing edges or fully elastic plates raise concerns about overall structural integrity, as the flexible plate may experience aeroelastic divergence or flutter [13]. These undesirable phenomena not only result in noise amplification but also jeopardize the system's overall aerodynamic performance and safety. Therefore, the practical application of existing noise control methods in real-world environments remains a challenging issue.

In this study, we propose a unique method to reduce trailing edge noise without the limitations of increased drag or aeroelastic flutter. The method involves the design of a structural compliance system with a finite number of elastic panels. Unlike concepts that involve a cantilever edge, the design preserves the structural integrity of the original trailing edge. Furthermore, the structural properties of the panels are set to align with the fluid-loaded natural frequencies which enable the panels to resonate structurally when exposed to incoming acoustic excitation.

2. PROBLEM SETUP AND NUMERICAL METHODOLOGY

The problem's physical arrangement aligns with Category 4 Problem 2 as presented in the Fourth Computational Aeroacoustics (CAA) Workshop on Benchmark Problems [14]. This setup is commonly used in various investigations focusing on trailing edge noise [9]. We consider flow over a semi-infinite thin rigid splitter plate with its trailing edge at the origin in two dimensions (Figure 1. The flow has a freestream Mach number $M = 0.2$ with a Reynolds number based on boundary layer momentum thickness θ as $Re_\theta = 530$. The thin splitter plate has a blunt end and a width of $h/\theta = 0.208$ which avoids any self-noise generation by trailing edge bluntness.

The proposed idea introduces embedded structural compliance, which involves replacement of multiple segments of plate with elastic panels. This modification aims to suppress noise scattering from the trailing edge of the plate. The length of all the elastic panels, denoted as L, is deliberately chosen to be very small ($\sim 90\theta$) as such short length is shorter than the dominant wavelength of convective flow fluctuations in the baseline flow, denoted as λ_{conv} (approximately 135θ). This ensures that the flow-induced vibration of any short panel does not act as an additional acoustic source, radiating energy to the far-field as confirmed by a recent study on the use of flow-induced vibrating panels for airfoil tonal noise suppression [7]. The compliance system, which encompasses the conceptual design, consists of three panels separated by $0.1L$ and positioned at a distance of $0.3L$ from the trailing edge. Each panel's edges are rigidly clamped. The panels are arranged with fluid-loaded panel resonant frequencies increasing (Config A) / decreasing (Config B) along the mean flow direction.

All the variables are considered in their dimensionless forms taking freestream flow properties (velocity $\hat{U}_\infty$, density ρ_∞, and temperature T_∞) and panel length $\hat{L}$ as reference, where the symbols with hat (^) denote their dimensional quantities. As such, the Reynolds number Re_L of the freestream is 5×10^4. In the present study, we adopt the direct aeroacoustics (DAS) approach for its capability of

resolving the inherent coupling between the unsteady aerodynamic and acoustic solutions with high accuracy. The problem is modeled by compressible Navier-Stokes (N-S) equations and the equation of state which govern all relevant aeroacoustic behaviors. The two-dimensional N-S equations can be written in strong conservative form as,

$$\frac{\partial \boldsymbol{U}}{\partial t} + \frac{\partial (\boldsymbol{F} - \boldsymbol{F}_v)}{\partial x} + \frac{\partial (\boldsymbol{G} - \boldsymbol{G}_v)}{\partial y} = 0, \tag{1}$$

where $\boldsymbol{U} = [\rho \quad \rho u \quad \rho v \quad \rho E]^T$, $\boldsymbol{F} = [\rho u \quad \rho u^2 + p \quad \rho uv \quad (\rho E + p)u]^T$, $\boldsymbol{F_v} = (1/Re)[0 \quad \tau_{xx} \quad \tau_{xy} \quad \tau_{xx}u + \tau_{xy}v - q_x]^T$, $\boldsymbol{G} = [\rho v \quad \rho uv \quad \rho v^2 + p \quad (\rho E + p)v]^T$ and $\boldsymbol{G_v} = (1/Re)[0 \quad \tau_{xy} \quad \tau_{yy} \quad \tau_{xy}u + \tau_{yy}v - q_y]^T$ are the flow flux conservation variables, ρ is the density of fluid, u and v are the velocities in x and y direction respectively, τ_{xx}, τ_{xy}, and τ_{yy} are the normal and shear stresses, q_x and q_y are the heat fluxes. The total energy and pressure are calculated by $E = p/\rho(\gamma - 1) + (u^2 + v^2)/2, p = \rho \mathrm{T}/\gamma M^2$. The non-dimensional time and frequency are defined by $t = \hat{t}\hat{U}_\infty/\hat{c}$ and $f = \hat{f}\hat{c}/\hat{U}_\infty$ respectively.

To solve the unsteady N-S equations, the conservation element and solution element (CE/SE) method is adopted. Details of its formulation and implementation are referred to [15]. The method has been successfully applied to analyze the complex aeroacoustic interactions at both external and internal subsonic flow problems [7, 16].

The computational domain is discretized into a structured mesh composed of 3200 x 1000 mesh elements. The mesh sizes around the plate trailing edge are carefully chosen to give minimum spacings of $\Delta x = 2 \times 10^{-4}$ and $\Delta y = 1.4 \times 10^{-4}$ respectively so as to ensure there are at least 14 mesh elements across the plate thickness. The mesh is smoothly stretched in the x and y directions away from the plate to save computational cost. In the application of the CE/SE scheme, a quadrangle mesh element is split into four triangles using diagonal cross divisions [15]. Hence a total mesh size of 1.4×10^7 elements is generated to accurately resolve the flow fluctuations propagating in the proximity to the plate and acoustic propagation to the far-field. Both sliding and no-slip boundary conditions are applied to the top and bottom surfaces of all plates. The transition point between these conditions is set in a way that allows the naturally developing boundary layer to achieve a prescribed Re_θ value of 530 at the plate's edge. Except for the inlet, buffer zones with exponentially stretching meshes are added to all open boundaries of the physical domain. These buffer zones are terminated with non-reflecting boundary conditions, as this approach effectively suppresses the propagation of erroneous numerical waves towards the interior of the domain. [17]. The time-marching process for solving Eq. 1 starts by using the steady solution to the compressible boundary layer equations. This steady solution has zero pressure gradient on both sides of the splitter plate. A time step size of $\Delta t = 1 \times 10^{-5}$ is employed, and the time evolution is carried out for a non-dimensional time duration of $t = 100$. The resulting time-stationary solution is considered as the baseline flow for further analysis.

To stimulate the natural flow instabilities within the laminar boundary layer, a weak broadband excitation is introduced to the solution. This excitation primarily aims to trigger scattering of the instabilities at the trailing edge of the flat plate, generating acoustic waves. The excitation is modeled as a monopole at $(x, y) = (-3.9, 0.02)$ with fluctuating pressure defined as $p'_{\mathrm{inc}} = p_A \sum_{k=1}^{50} \sin(2\pi t f_{\mathrm{exc},k} + \phi_k)$, where $p_A = 10^{-5}$. The excitation frequencies cover $1.5 \leq f_{\mathrm{exc},k} \leq 5$ with random phases ϕ_k. Such choice allows at least one wavelength of scattered noise at the lowest excitation frequency can be captured yet the shortest excitation wavelength can be accurately resolved by the mesh.

The nonlinear dynamic response of an elastic panel is modeled by solving the one-dimensional plate equation to its simplest approximation [18]. The governing equation for panel displacement, normalized by aforementioned flow reference variables, can be written as,

$$S_{\mathrm{P}} \frac{\partial^4 w}{\partial x^4} - (T_{\mathrm{P}} + N_{\mathrm{P}}) \frac{\partial^2 w}{\partial x^2} + \rho_{\mathrm{P}} h_{\mathrm{P}} \frac{\partial^2 w}{\partial t^2} + C_{\mathrm{P}} \frac{\partial w}{\partial t} + K_{\mathrm{P}} w = p_{\mathrm{ex}} \tag{2}$$

where w is the panel displacement from its undisturbed position, S_{P} is the panel bending stiffness, T_{P} is the external tensile stress in tangential direction, h_{P} is thickness of panel, N_{P} is the internal

tensile stress in the tangential direction, C_P is the structural damping coefficient of the panel, K_P is the stiffness of the foundation supporting the panel and p_{ex} is the net pressure acting across panel surfaces [7]. The nonlinear coupling between aeroacoustic fluctuation and panel structural dynamics is resolved with a monolithic scheme [19].

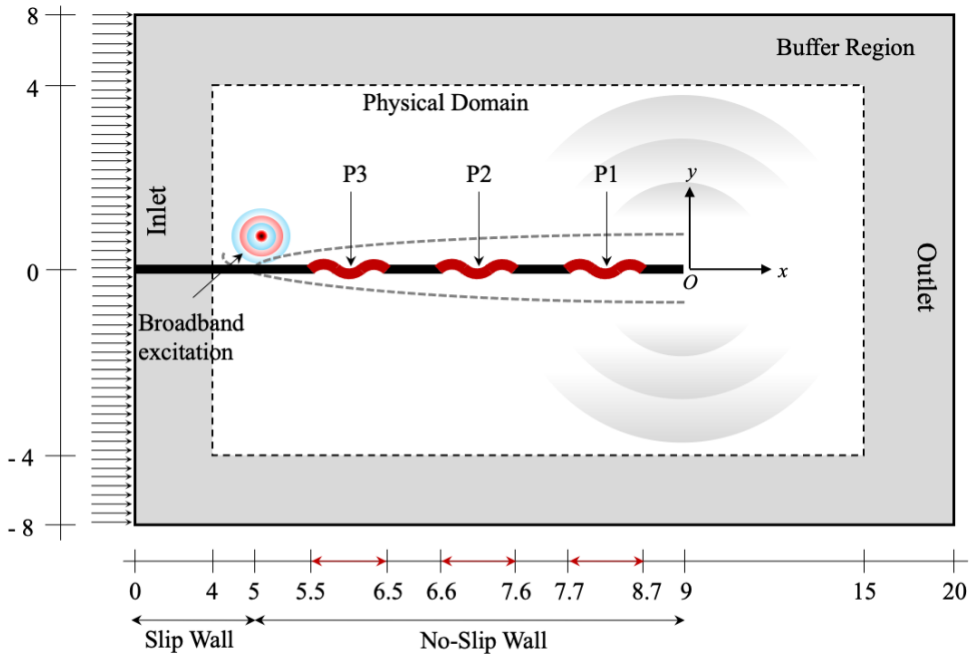

Figure 1: Schematic sketch of the computational domain.

An essential condition for the proposed concept is to carefully select the structural properties of the panels, including density, thickness, and external tension. These properties must be chosen in such a way that the natural frequencies of the panels, when subjected to fluid loading, align with the frequencies of the incident and scattered noise as well as flow fluctuations. The normalized frequency of the n^{th} vibration mode of a panel can be estimated using formulas provided in previous studies [20].

$$(f_P)_n = \frac{n}{2L_P}\sqrt{\frac{T_P}{\rho_P h_P}}\sqrt{1+\frac{L_P}{\pi n \rho_P h_P}}\,. \tag{3}$$

where L_P is the length of panel. In the present study the three elastic panels P1, P3 and P2 are set to give flow-induced structural resonance respectively at the lowest frequency $f = 1.5$, the highest frequency $f = 5.0$, and their arithmetic mean ($f = 3.25$) of the excitation. Details of panel properties are presented in Table 1.

Table 1: Designed panel parameters.

Panel	Coverage (x-direction) Config A / Config B	Material	Density ρ_P	Resonant frequency f_P	Resonant mode n
P1	-3.5 to -2.5 / -1.3 to -0.3	Stainless Steel	6367.34	1.5	2
P2	-2.4 to -1.4 / -2.4 to -1.4	Carbon Fiber	2212.24	3.25	3
P3	-1.3 to -0.3 / -3.5 to -2.5	Silicon Rubber	833.45	5.0	3

3. RESULTS AND DISCUSSION

3.1. Near Field Analysis

Figure 2 presents a comparison of the streamwise distributions of scattered pressure fluctuations observed on the upper surface of the splitter plate. To obtain these distributions, we subject the temporal flow pressure fluctuations recorded at various locations along the plate surface to Fast Fourier Transform (FFT). This process allows us to extract their spectral amplitudes, characteristic frequencies, and their distribution along the streamwise direction. The spectra shown in the figure are calculated over a duration of $t = 10$, using a high sampling frequency of 1×10^5.

From Figure 2, it becomes apparent that each panel not only resonates to absorb flow energy at its designed frequency but also absorbs energy at other frequencies as well. The combined effects of all the panels contribute to the effective suppression of broadband flow instability. For Config A, we observe a noticeable reduction in boundary layer instability at each designed panel frequency compared to the rigid plate solution. Figure 2(a) demonstrates a sharp suppression of boundary layer instability over panel P1 at $f = 1.5$, resulting from the flow-induced resonance of the panel. Although relatively weaker, the subsequent suppression by two downstream panels can be observed over panel P2 at $f = 3.25$ and over panel P3 at $f = 5$. As a result, an effective overall suppression of flow scattering at the trailing edge is achieved for Config A. Interestingly, when the arrangement of panel installation is reversed (Config B), the overall suppression becomes less effective.

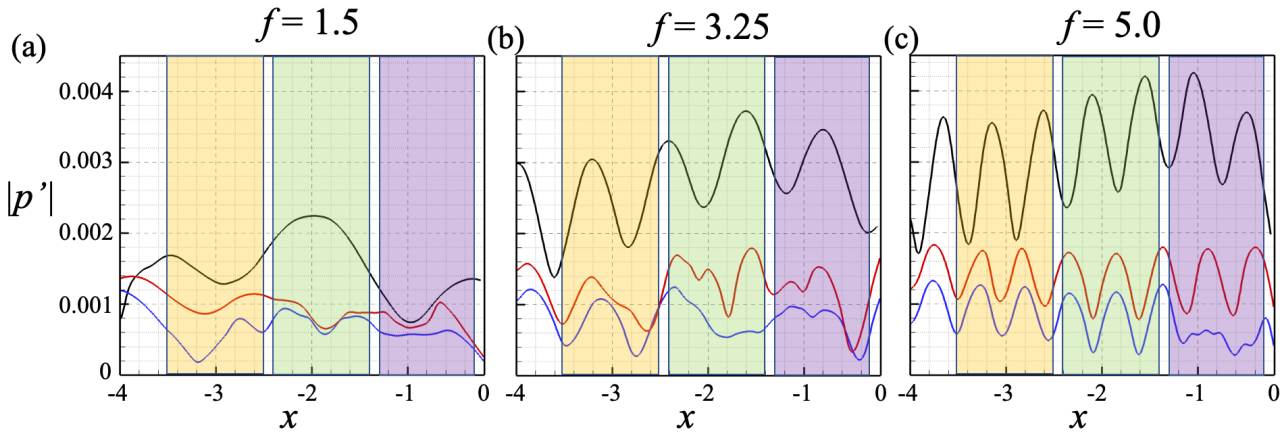

Figure 2: (a)-(c) Streamwise distributions of scattered pressure fluctuation magnitudes on splitter plate upper surface. The shaded areas indicate the coverage of panels. ——, Rigid plate; ——, Config A; ——, Config B.

Figure 3 shows that the scattering suppression effectiveness is significantly higher for Config A, with an overall reduction in the magnitude of p' (pressure fluctuations) of approximately 65% compared to approximately 52% for Config B. This difference can be attributed to the varying extent of continuous reduction at panel resonant frequencies in the two systems (Figures 3(a)-(c)). These observations indicate that a compliance system with panels embedded with increasing resonance frequencies is more effective in noise suppression than its other counterpart.

3.2. Acoustic Analysis

We now examine the impact of the embedded compliance systems on the scattering of trailing edge noise. To evaluate the extent of noise suppression, we analyze the azimuthal distribution p'_{rms} at a radius of $r = 3$ from the trailing edge of the plate. Figure 4 present the p'_{rms} distribution for both compliance systems along with their comparison with rigid splitter plate. It is evident that the reduction in p'_{rms} above the splitter plate is significantly higher than below. In both configurations,

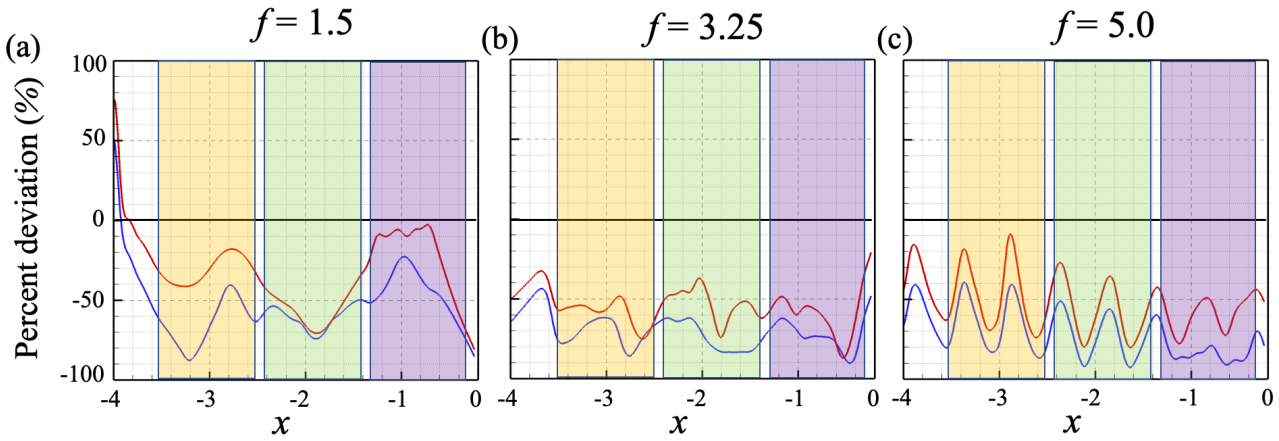

Figure 3: (a)-(c) Relative deviation in fluctuation amplitudes to the case of rigid plate. The shaded areas indicate the coverage of panels. ——, Rigid plate; ——, Config A; ——, Config B.

the maximum reduction occurs within the sector $60^o \leq \theta \leq 120^o$. For both configurations, a similar azimuthal distribution is observed, but with weaker in p'_{rms} for Config B as compared to Config A.

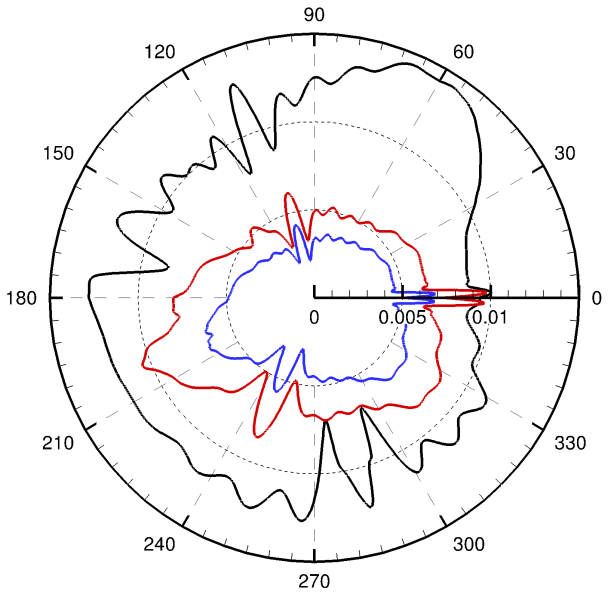

Figure 4: Azimuthal distribution of p'_{rms} at a radius of $r = 3$ from the trailing edge of the plate. ——, Rigid plate; ——, Config A; ——, Config B.

Figures 5(a) and (b) illustrate the acoustic spectra recorded just above and below the trailing edge, clearly demonstrating the suppression of noise scattering. Config A shows a relatively uniform sound pressure level SPL reduction of 10 dB across the entire frequency range of interest. On the other hand, Config B exhibits lower reduction, particularly at low to mid frequencies, resulting in a lower overall reduction. These observations support the notion that the compliance systems effectively absorb the energy of flow instabilities before scattering occurs at the trailing edge of the splitter plate.

3.3. Panels Vibrational Analysis

To analyze the dynamic behaviors of the panels, we examine the spatio-temporal evolution of the panel displacements (Figures 6(a) and (b)). In each case, the time-stationary solution is captured and analyzed in a time-synchronized manner. The spatio-temporal variations of the panel

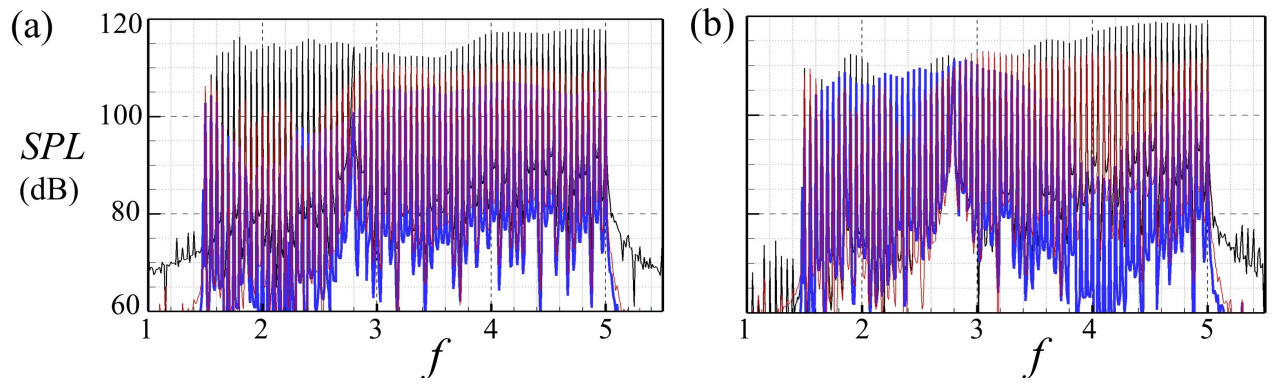

Figure 5: (a) and (b), Acoustic pressure spectra captured at $(x, y) = (0, 3)$ and $(x, y) = (0, -3)$ respectively. ——, Rigid plate; ——, Config A; ——, Config B.

displacements (w) for Config A indicate that all panels are able to sustain their designed resonant modes around $w = 0$, and their corresponding standing wave patterns on the panels are evident (Figure 6(a)). Panel P1 exhibits a more regular standing wave pattern compared to P2 and P3, suggesting a more coherent energy transfer from flow fluctuations that sustains its vibration over the longer resonant wavelength of P1. The low displacement amplitudes of the panels indicate that the mean flow characteristics remain unaffected by panel dynamics.

In contrast, the panel responses of Config B differ from Config A (Figure 6(b)). The upstream panel (P3) is unable to vibrate in its designed resonant mode, and the same applies to the two downstream panels. Panel P3 vibrates with a maximum displacement comparable to the boundary layer thickness. This may lead to distortion of the mean flow characteristics, potentially adversely affecting the flow-panel coupling of P2 and P1 downstream. Consequently, the maximum displacements of P2 and P1 are at least one order of magnitude weaker than P3.

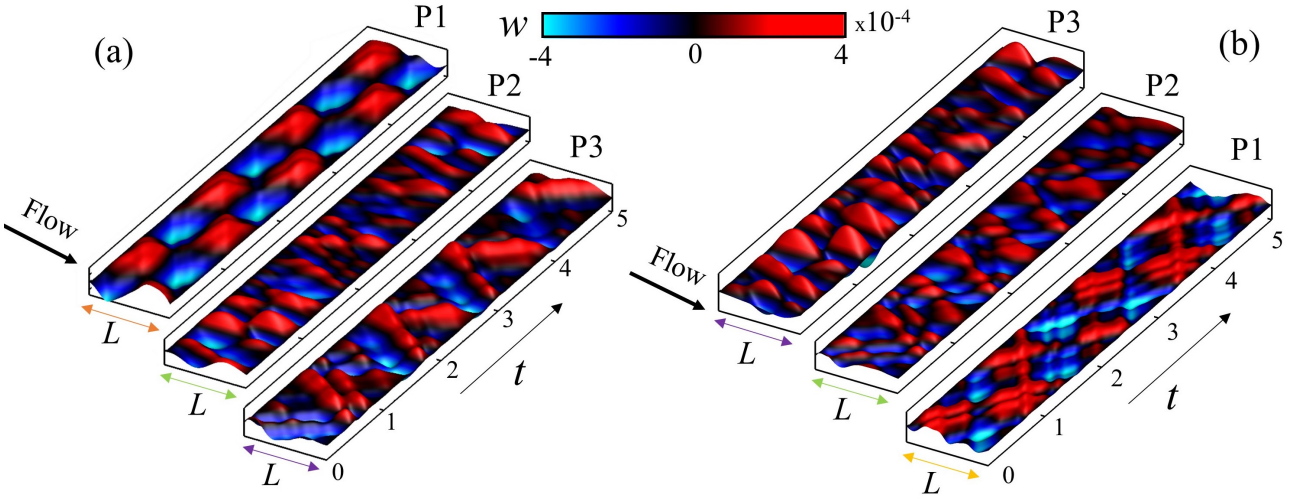

Figure 6: Spatio-temporal evolution of panel center vibration. (a) Config A and (b) Config B.

4. CONCLUSIONS

A unique method for the reduction in flow-induced trailing edge noise scattering for a semi-infinite thin plate is proposed by utilizing short flexible panels mounted on the surface of the plate. The proposed concept involves the incorporation of a compliance system consisting of three rigidly clamped elastic panels. This compliance system aims to absorb the energy of incident flow fluctuations by utilizing the panel's structural resonance, achieved by matching the fluid-loaded

panel's natural frequencies with the frequency range of interest for noise reduction. The feasibility of the concept is investigated through high-fidelity direct aeroacoustic simulations, coupled with spatio-temporal analysis of aeroacoustic-structural interactions. The structural analysis shows a systematic vibration pattern for all the panels which clearly indicates the presence of complex fluid-structural interaction under resonance conditions.

ACKNOWLEDGEMENTS

The authors gratefully acknowledge the support from the Research Grants Council of the Government of Hong Kong Special Administrative Region under grant number 15208520.

REFERENCES

1. Irsalan Arif, G. C. Y. Lam, Di Wu, and R. C. K. Leung. Passive airfoil tonal noise reduction by localized flow-induced vibration of an elastic panel. *Aerospace Science and Technology*, 107:106319, 2020.
2. Thomas F Brooks and TH Hodgson. Trailing edge noise prediction from measured surface pressures. *Journal of sound and vibration*, 78(1):69–117, 1981.
3. Michel Roger and Stéphane Moreau. Broadband self noise from loaded fan blades. *AIAA journal*, 42(3):536–544, 2004.
4. G Desquesnes, M Terracol, and P Sagaut. Numerical investigation of the tone noise mechanism over laminar airfoils. *Journal of Fluid Mechanics*, 591:155–182, 2007.
5. N Curle. The influence of solid boundaries upon aerodynamic sound. *Proceedings of the Royal Society of London. Series A. Mathematical and Physical Sciences*, 231(1187):505–514, 1955.
6. Jing Wang, Chengchun Zhang, Zhengyang Wu, James Wharton, and Luquan Ren. Numerical study on reduction of aerodynamic noise around an airfoil with biomimetic structures. *Journal of Sound and Vibration*, 394:46–58, 2017.
7. Irsalan Arif, Di Wu, G. C. Y. Lam, and R. C. K. Leung. Exploring airfoil tonal noise reduction with elastic panel using perturbation evolution method. *AIAA Journal*, 58(11):4958–4968, 2020.
8. Laura Kamps, Christoph Brücker, Thomas F Geyer, and Ennes Sarradj. Airfoil self noise reduction at low reynolds numbers using a passive flexible trailing edge. In *23rd AIAA/CEAS Aeroacoustics Conference*, page 3496, 2017.
9. Youngmin Bae, Jae Young Jang, and Young J Moon. Effects of fluid-structure interaction on trailing-edge noise. *Journal of mechanical science and technology*, 22(7):1426–1435, 2008.
10. Massimiliano Nardini, Richard D Sandberg, and Stefan C Schlanderer. Computational study of the effect of structural compliance on the noise radiated from an elastic trailing-edge. *Journal of Sound and Vibration*, 485:115533, 2020.
11. AVG Cavalieri, WR Wolf, and JW Jaworski. Numerical solution of acoustic scattering by finite perforated elastic plates. *Proceedings of the Royal Society A: Mathematical, Physical and Engineering Sciences*, 472(2188):20150767, 2016.
12. Elena Kolb and Michael Schaefer. Aeroacoustic simulation of flexible structures in low mach number turbulent flows. *Computers & Fluids*, 227:105020, 2021.
13. Earl H Dowell. *Aeroelasticity of plates and shells*, volume 1. Springer Science & Business Media, 1974.
14. Milo D Dahl. Fourth computational aeroacoustics (caa) workshop on benchmark problems. In *Fourth Computational Aeroacoustics (CAA) Workshop on Benchmark Problems*, number NASA/CP—2004-212954, 2004.

15. G. C. Y. Lam, R. C. K. Leung, K. H. Seid, and S. K. Tang. Validation of CE/SE scheme in low mach number direct aeroacoustic simulation. *International Journal of Nonlinear Sciences and Numerical Simulation*, 15(2):157–169, 2014.
16. G. C. Y. Lam and R. C. K. Leung. Aeroacoustics of NACA 0018 airfoil with a cavity. *AIAA Journal*, 56(12):4775–4786, 2018.
17. Irsalan Arif, G. C. Y. Lam, and R. C. K. Leung. Coupled structural resonance of elastic panels for suppression of airfoil tonal noise. *Journal of Fluids and Structures*, 110:103506, 2022.
18. MR Visbal and RE Gordnier. Numerical simulation of the interaction of a transitional boundary layer with a 2-D flexible panel in the subsonic regime. *Journal of Fluids and Structures*, 19(7):881–903, 2004.
19. H. K. H. Fan, R. C. K. Leung, G. C. Y. Lam, Yves Aurégan, and Xiwen Dai. Numerical coupling strategy for resolving in-duct elastic panel aeroacoustic/structural interaction. *AIAA Journal*, 56(12):5033–5040, 2018.
20. Robert D Blevins and R Plunkett. Formulas for natural frequency and mode shape. *Journal of Applied Mechanics*, 47(2):461, 1980.